Colloidal Quantum Dots as Saturable Fluorophores

Osip Schwartz,* Ron Tenne, Jonathan M. Levitt, Zvicka Deutsch, Stella Itzhakov, and Dan Oron

Department of Physics of Complex Systems, Weizmann Institute of Science, Rehovot, Israel 76100

ABSTRACT Although colloidal quantum dots (QDs) exhibit excellent photostability under mild excitation, intense illumination makes their emission increasingly intermittent, eventually leading to photobleaching.

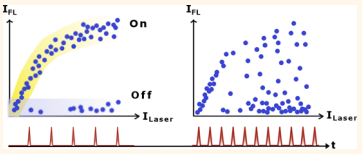

We study fluorescence of two commonly used types of QDs under pulsed excitation with varying power and repetition rate. The photostability of QDs is found to improve dramatically at low repetition rates, allowing for prolonged optical saturation of QDs without apparent photodamage. This observation suggests that QD blinking is facilitated by absorption of light in a transient state with a microsecond decay time. Enhanced photostability of generic quantum dots under intense illumination opens up new prospects for fluorescence microscopy and spectroscopy.

KEYWORDS: quantum dot blinking · saturable fluorescence · fluorophore photostability

Fluorescent labels, such as organic dyes and quantum dots, are universally employed in life science applications such as microscopy and single-molecule spectroscopy. Many of these applications depend critically on photostability of the fluorophores; for example, confocal or multiphoton microscopy modalities often require intense illumination.[1,2] Moreover, a number of super-resolved microscopy techniques rely on fluorophore saturation.[3−5] Quantum imaging also requires observing fluorophores at or beyond the saturation threshold.[6] However, most organic fluorophores in a bioenvironment are susceptible to photodamage even at powers much below saturation, producing a given maximal number of photons before photobleaching.[7] Although QDs typically demonstrate better photostability than most organic dyes,[8−10] their emission is usually steady only at powers well below saturation, with increased blinking followed by photobleaching at high excitation powers.[11,12]

Recently, it was demonstrated that blinking can be mitigated or eliminated by controlling the chemical environment of QDs,[13,14] by engineering QDs with smooth effective potential,[15] or by overcoating the QDs with very thick insulating shells.[16,17] The first two approaches, however, were demonstrated only at relatively low excitation power. On the other hand, the giant QDs of refs 16 and 17 were shown to remain nonblinking even under optical saturation conditions.[18] These nanocrystals demonstrate behavior intermediate between regular QDs and bulk semiconductor crystals, with typical fluorophore features such as photon antibunching and fluorescence saturation less pronounced due to reduced Auger interactions.[19] Their relatively large size might, however, present an obstacle for some applications.

It has been shown previously that utilizing pulsed illumination with microsecond intervals between pulses can substantially improve the total photon yield of organic dyes, which was attributed to suppression of the triplet state mediated photobleaching.[20,21] At the same time, the pioneering work by Nirmal *et al.*[22] associated QD blinking with a two-step ionization process involving a trap state with a lifetime of about 5 μs. On the other hand, recent studies suggest that QD blinking is due to rapid charge carrier capture by a trap state, active during the "off" intervals but dormant during the "on" times.[23−25] It might be conjectured that, similarly to the triplet state absorption role in photobleaching of organic dyes, absorbing a photon while the trap state is occupied can facilitate photodamage. Under this assumption, the presence of a trap state and its decay time can be established by examining the dependence of the QD photostability on the excitation repetition rate. While the power dependence of QD blinking properties has received some attention,[18,26,27] the effects of the repetition rate on the QD photostability have not been addressed yet.

In this work, we examine blinking properties of individual QDs, studying their fluorescence emission at various repetition rates and at excitation power ranging from

* Address correspondence to osip.schwarz@weizmann.ac.il.

Received for review June 10, 2012 and accepted September 19, 2012.

Published online September 19, 2012
10.1021/nn302551v

the linear regime and well into saturation. We demonstrate that photostability of generic quantum dots, exhibiting regular blinking properties and susceptible to photodamage under usual conditions, is improved dramatically under pulsed illumination with low repetition rates.

In our experiments, we used two well-studied[28] and commonly used types of QDs: CdSe/CdS/ZnS core–shell–shell QDs and CdSe/CdS seeded nanorods[29] (see Supporting Information for additional details).

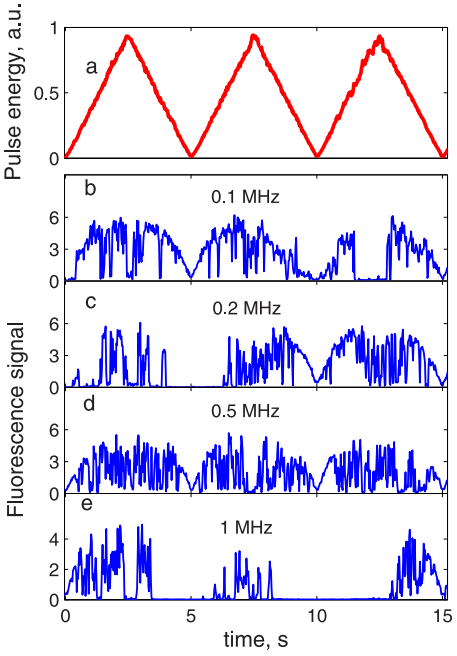

Figure 1. (a) Measured excitation pulse energy as a function of time. (b–e) Example traces of fluorescent signal from a CdSe/CdS nanorod as a function of time, at the repetition rates of 100 kHz to 1 MHz. Fluorescence signal is in the units of photon counts per 100 excitation pulses.

RESULTS AND DISCUSSION

To investigate fluorescence saturation behavior of individual QDs, we conducted the following experiment. The fluorescence signal was collected continuously from single nanocrystals, while the pulse energy was gradually changed with time following a triangular wave pattern, as shown in Figure 1a, and the repetition rate was kept constant. Such measurements were conducted on the same nanocrystal at several repetition rates. A typical fluorescence trace from an individual CdSe/CdS nanorod is shown in Figure 1b–e. The general flat-top shape of the signal curves indicates QD saturation. Similar height of all peaks shows that QDs did not undergo photodamage in the relevant time scale. A higher proportion of dark periods is evident at higher repetition rates.

Traces similar to those shown in Figure 1b–e were time-binned to produce signal *versus* excitation power scatter plot diagrams shown in Figure 2. Each scatter plot is shown together with a histogram of the QD brightness probability distribution corresponding to a given range of excitation power. The figure shows data from three typical QDs studied at repetition rates ranging from 100 kHz to 1 MHz.

At low pulse energy and low repetition rates, most data points fall on the same line. With increasing pulse energy, the scatter increases significantly. Nevertheless, at low repetition rates, most data points cluster around a clear saturation curve. As the interpulse intervals are decreased, more and more data points are shifted downward from the curve due to emission intermittency, so at the highest repetition rate the time-averaged signal almost disappears. The fluorescence intermittency dependence on the repetition rate is seen clearly in the QD brightness histograms. At the lowest repetition rate, the histograms demonstrate a

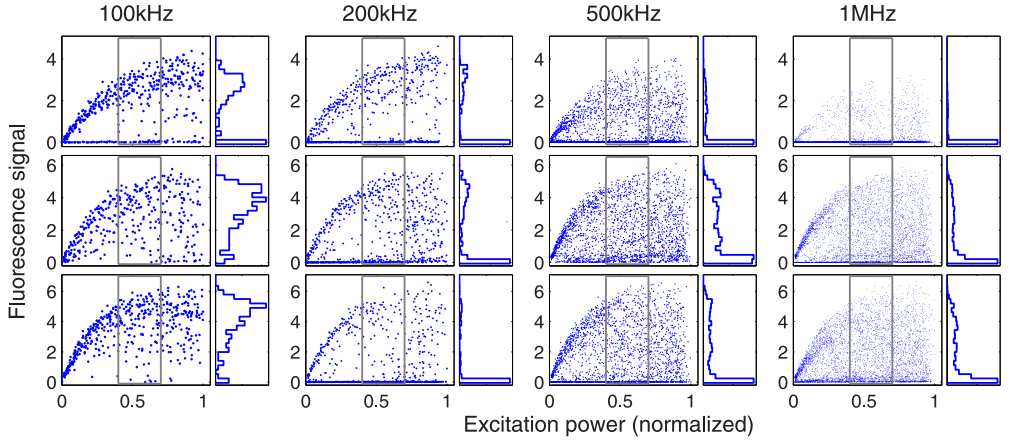

Figure 2. CdSe/CdS nanorod saturation behavior dependence on the excitation repetition rate. Every row of panels corresponds to a single CdSe/CdS nanorod, while each column represents data at a given repetition rate. Each panel shows a scatter plot diagram of a fluorescence signal against excitation pulse energy, accompanied by a histogram of QD brightness distribution built from the data in the framed area in the scatter plots (gray rectangles). The fluorescence signal is given in the units of photons detected per 100 pulses, representing the cumulative efficiency comprising the efficiency of QD excitation, emission, optical collection efficiency, and detector quantum efficiency. The vertical scale is the same for all panels in one row. The pulse energy is given in normalized units, the maximal pulse energy corresponding to a fluence of 80 μJ/cm^2.

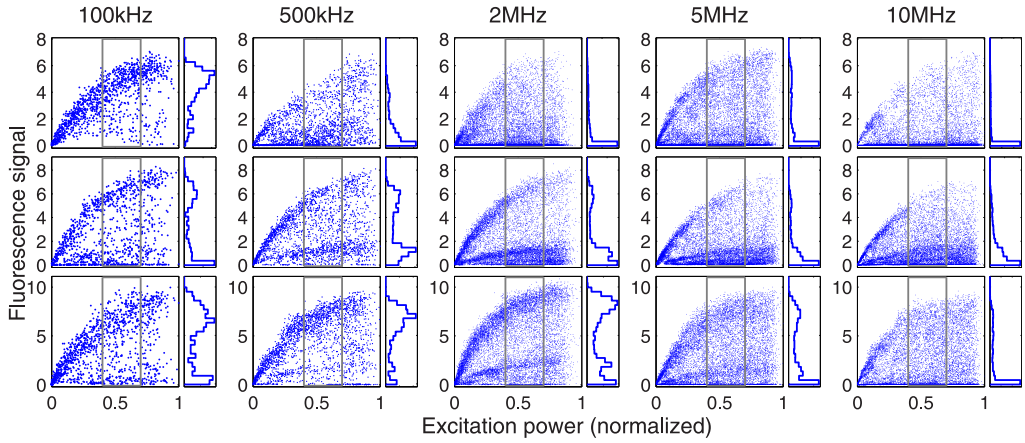

Figure 3. CdSe/CdS/ZnS QD saturation curve dependence on the repetition rate. As in Figure 2, every row in a panel corresponds to a single QD, while each column represents data at a given repetition rate. The fluorescence signal is given in the units of photons detected per 100 pulses. The data were time-gated by discarding the photons arriving in the first 5 ns after the excitation pulse. The pulse energy is given in normalized units, the maximal pulse energy corresponding to a fluence of 50 μJ/cm^2.

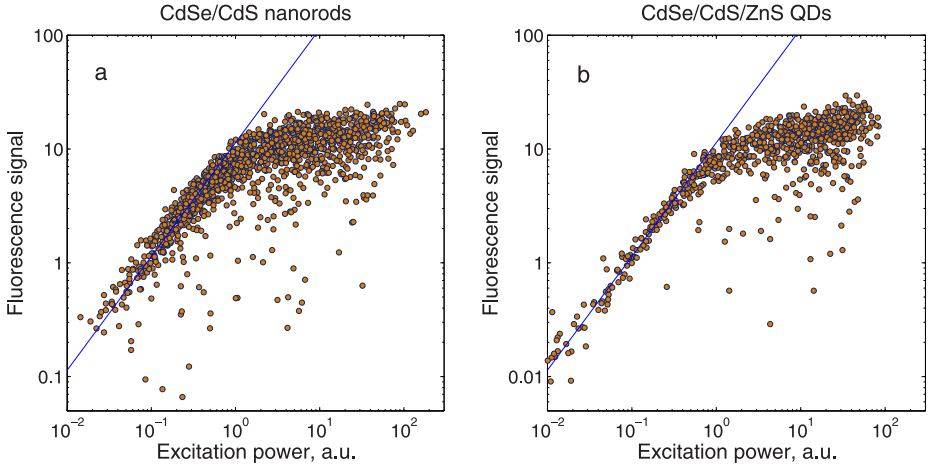

Figure 4. QD fluorescence brightness as a function of the excitation power, recorded at a repetition rate of 1 kHz using a CCD, in log−log scale. (a) Data for 24 CdSe/CdS nanorods and (b) 26 individual CdSe/CdS/ZnS QDs. The signal axis is graduated in the units of photons detected per 100 excitation pulses. The excitation power was scaled for every QD to give the same slope in the linear part of the saturation curve, accounting for the variations of local excitation intensity and variations of the cross sections. The trend lines correspond to the linear dependence of signal on excitation power.

wide peak corresponding to the on state, occasionally also featuring a narrow off state peak at zero signal, which corresponds to almost continuous emission with moderate blinking. As the repetition rate is increased, the brightness distributions become wider and shift to lower signals, corresponding to increased fluorescence intermittency, while the zero-signal peak grows. At the highest repetition rate of 1 MHz, the QDs spend a significant fraction of time in the off state, and the average signal per excitation pulse is drastically reduced compared to the signal at low repetition rates.

The results of a similar experiment conducted on CdSe/CdS/ZnS QDs are shown in Figure 3. The figure presents saturation scatter plots for three typical QDs at repetition rates varying from 100 kHz to 10 MHz. Each of the three rows of the figure correspond to a single nanocrystal. Unlike nanorods, the CdSe/CdS/ZnS QDs feature a relatively high biexciton quantum yield (BXQY) of ~20%, which makes the saturation less pronounced. To take into account only the single-exciton signal, we discard all photons arriving in the first 5 ns after the excitation pulse. The effect of such time gating on the saturation curves and BXQY derivation for both kinds of QDs are described in the Supporting Information. The scatter plots and histograms shown in Figure 3 show the same trends as those of Figure 2, demonstrating in addition to the on and off states also "gray" states with reduced quantum yield.

While the average signal decreases with the repetition rate, the autocorrelation analysis of fluorescence traces of both types of QDs shows dramatic shrinking of typical durations of blinking events (see Supporting Information for details).

To extend our study to even longer interpulse intervals, we utilized a wide-field fluorescence imaging setup operating at 1 kHz (see Methods section). The combined saturation curves of 24 individual CdSe/CdS nanorods and 26 CdSe/CdS/ZnS QDs are shown in Figure 4 in log−log scale. To account for uneven optical

power density across the field of view and variations of the absorption, the excitation power was normalized so that four lowest-power points of each saturation curve correspond to the same slope. No adjustment was made to the vertical scale of the plots. Both types of QDs demonstrate saturation brightness of about 0.1 detected photon per excitation pulse, which, to our knowledge, is the highest efficiency reported to date for fluorophores that can be utilized as labels for bioimaging.

Similarly to Figures 2 and 3, at low power, the data points fall on the same line (although, in contrast to Figures 2 and 3, these represent the combined data from many QDs). The plots show a sharp bend at the saturation threshold, followed by a period of much slower growth, extending for about two decades. The excitation power in these plots was limited by the available laser power, corresponding to a fluence of $\sim$1.2 mJ/cm^2. The vertical dispersion of the data points is due to both the differences in brightness between individual QDs and the fluorescence intermittency. Although the dispersion increases significantly after the bend, the average signal is not significantly affected by blinking even at high power. Indeed, no degradation of QDs was observed during 1 h of continuous illumination at the highest excitation intensity used to obtain the data of Figure 4 (see Supporting Information for further details). These plots show that deep saturation of QDs, up to a factor of about 50, is possible at 1 kHz repetition rate with very little fluorescence intermittency and without inflicting permanent damage. The sharp decrease of QD blinking at low repetition rates demonstrates that the excitation power and repetition rate dependence are key aspects of QD fluorescence intermittency, suggesting that QD photostability and (non)blinking properties should be assessed relating to given excitation conditions.

The rapid signal fluctuations observed at high repetition rates suggest a stochastic, excitation pulse-driven model of the on−off transitions. At the same time, the change in blinking behavior taking place at the interpulse intervals of several microseconds for CdSe/CdS nanorods and about 1 μs for CdSe/CdS/ZnS QDs implies that, at least with a certain probability, the processes initiated in a QD by the excitation pulse do not decay completely in the corresponding time scale, almost 2 orders of magnitude longer than radiative decay time in these QDs.

This memory effect can be interpreted as the decay time of the trap state responsible for photodarkening. Exploring the properties of such trap states is essential for understanding of blinking processes in QDs. At present, their most studied parameter is the trapping rate, which was estimated by Zhao *et al.*[23] to be less than 1/100 of the radiative time, corresponding to a few hundred picoseconds, while the distributions of trapping rate measured in ref 24 for CdSe/CdS/ZnS QDs were centered around 250 ps, largely independent of the QD size. On the other hand, in ref 25, it is found that a hot electron can be trapped before cooling to the band edge, which requires a trapping rate faster than the intraband relaxation rate. Another important parameter of the trap states, the decay time, was estimated in ref 24 to be on the order of a few hundred nanoseconds, which agrees well with the 1 μs characteristic time scale reported here. Overall, the repetition rate dependence of the fluorescence intermittency corroborates the model of QD blinking *via* charge carrier capture by a transient trap state and provides a measure of the decay time of such states.

Currently, a major limitation in saturation-based super-resolution microscopy[3,4] is the lack of a biocompatible fluorophore able to withstand deep saturation long enough to allow for sufficient amount of fluorescent photons to be collected. Our results can provide a solution to this problem, enabling regular QD fluorescent labels to serve as saturable fluorophores resilient to photodamage. Although it seems natural to assume that imaging QDs at low repetition rates must entail very long signal accumulation, it is not necessarily so. For example, in a scanning confocal or two-photon microscope, the beam can be scanned so fast that every diffraction-limited spot will be exposed to an excitation pulse only once per scan, so that the necessary long intervals between pulses are filled by exciting the fluorophores at different parts of the sample.[20] In this setting, it should be possible to take advantage of the bright signal emitted by QDs near their saturation threshold without inflicting photodamage.

CONCLUSION

We have shown that regular QDs, not possessing any special nonblinking properties, become remarkably photostable at sufficiently low repetition rates, despite deep saturation. This observation sheds new light on the QD blinking mechanism, suggesting that a central role in photodarkening is played by a long-lived transient state. The resulting ability to saturate regular QDs without inflicting photodamage can be beneficial for fluorescence spectroscopy and microscopy modes requiring high excitation fluence.

METHODS

In the individual nanocrystal experiments, the QDs were embedded in a poly(methyl methacrylate) film spin-coated onto a glass coverslip. Fluorescence was excited using a variable repetition rate 470 nm mode-locked laser with a pulse duration of 100 ps (Edinburgh Instruments). The excitation light was focused on individual QDs using a 63× oil immersion objective with NA of 1.4, which was also used to collect the emitted light. The fluorescence signal was split between two channels using a multimode fiber splitter and directed into a pair of avalanche photodiodes (Perkin-Elmer),

connected to a time-correlated single-photon counting module (PicoQuant HydraHarp 400).

For the wide-field experiment, we used a 532 nm Q-switched laser emitting 300 ps pulses at a repetition rate of 1 kHz. Fluorescent signal was detected by an electron-multiplying charge-coupled device (CCD). The fluorescence signal from individual QDs was calculated as the sum of the CCD readings, converted to the units of photoelectrons, over computer-identified areas in the image corresponding to individual QDs. The background, estimated as the median pixel reading in the vicinity of every dot at a given excitation power, was subtracted from the fluorescence signal.

Conflict of Interest: The authors declare no competing financial interest.

Acknowledgment. Financial support by the European Research Council starting investigator Grant SINSLIM 258221 and by the Crown center of photonics is gratefully acknowledged. O.S. is supported by the Adams Fellowship Program of the Israel Academy of Science and Humanities. D.O. is the incumbent of the Recanati career development chair in energy research.

Supporting Information Available: Detailed description of the synthesis process, antibunching measurements and biexciton quantum yield; decay curves and temporal filtering; blinking statistics, and long-term photostability. This material is available free of charge *via* the Internet at http://pubs.acs.org.

REFERENCES AND NOTES

1. Denk, W.; Strickler, J.; Webb, W. Two-Photon Laser Scanning Fluorescence Microscopy. *Science* **1990**, *248*, 73–76.
2. Wilson, T. *Confocal Microscopy*; Academic Press: London, 1990; Vol. 426, pp 1−64.
3. Gustafsson, M. G. L. Nonlinear Structured-Illumination Microscopy: Wide-Field Fluorescence Imaging with Theoretically Unlimited Resolution. *Proc. Natl. Acad. Sci. U.S.A.* **2005**, *102*, 13081–13086.
4. Fujita, K.; Kobayashi, M.; Kawano, S.; Yamanaka, M.; Kawata, S. High-Resolution Confocal Microscopy by Saturated Excitation of Fluorescence. *Phys. Rev. Lett.* **2007**, *99*, 228105.
5. Heintzmann, R.; Jovin, T. M.; Cremer, C. Saturated Patterned Excitation Microscopy—A Concept for Optical Resolution Improvement. *J. Opt. Soc. Am. A* **2002**, *19*, 1599–1609.
6. Schwartz, O.; Oron, D. Improved Resolution in Fluorescence Microscopy Using Quantum Correlations. *Phys. Rev. A* **2012**, *85*, 033812.
7. Tsien, R.; Ernst, L.; Waggoner, A. Fluorophores for Confocal Microscopy: Photophysics and Photochemistry. In *Handbook of Biological Confocal Microscopy*; Pawley, J. B., Ed.; Springer: New York, 2006; pp 338−352.
8. Resch-Genger, U.; Grabolle, M.; Cavaliere-Jaricot, S.; Nitschke, R.; Nann, T. Quantum Dots *versus* Organic Dyes as Fluorescent Labels. *Nat. Methods* **2008**, *5*, 763–775.
9. Larson, D. R.; Zipfel, W. R.; Williams, R. M.; Clark, S. W.; Bruchez, M. P.; Wise, F. W.; Webb, W. W. Water-Soluble Quantum Dots for Multiphoton Fluorescence Imaging *in Vivo*. *Science* **2003**, *300*, 1434–1436.
10. Michalet, X.; Pinaud, F. F.; Bentolila, L. A.; Tsay, J. M.; Doose, S.; Li, J. J.; Sundaresan, G.; Wu, A. M.; Gambhir, S. S.; Weiss, S. Quantum Dots for Live Cells, *In Vivo* Imaging, and Diagnostics. *Science* **2005**, *307*, 538–544.
11. Lounis, B.; Bechtel, H.; Gerion, D.; Alivisatos, P.; Moerner, W. Photon Antibunching in Single CdSe/ZnS Quantum Dot Fluorescence. *Chem. Phys. Lett.* **2000**, *329*, 399–404.
12. van Sark, W. G. J. H. M.; Frederix, P. L. T. M.; Van den Heuvel, D. J.; Gerritsen, H. C.; Bol, A. A.; van Lingen, J. N. J.; de Mello Doneg, C.; Meijerink, A. Photooxidation and Photobleaching of Single CdSe/ZnS Quantum Dots Probed by Room-Temperature Time-Resolved Spectroscopy. *J. Phys. Chem. B* **2001**, *105*, 8281–8284.
13. Hohng, S.; Ha, T. Near-Complete Suppression of Quantum Dot Blinking in Ambient Conditions. *J. Am. Chem. Soc.* **2004**, *126*, 1324–1325.
14. Antelman, J.; Ebenstein, Y.; Dertinger, T.; Michalet, X.; Weiss, S. Suppression of Quantum Dot Blinking in DTT-Doped Polymer Films. *J. Phys. Chem. C* **2009**, *113*, 11541–11545.
15. Wang, X.; Ren, X.; Kahen, K.; Hahn, M.; Rajeswaran, M.; Maccagnano-Zacher, S.; Silcox, J.; Cragg, G.; Efros, A.; Krauss, T. Non-blinking Semiconductor Nanocrystals. *Nature* **2009**, *459*, 686–689.
16. Chen, Y.; Vela, J.; Htoon, H.; Casson, J. L.; Werder, D. J.; Bussian, D. A.; Klimov, V. I.; Hollingsworth, J. A. "Giant" Multishell CdSe Nanocrystal Quantum Dots with Suppressed Blinking. *J. Am. Chem. Soc.* **2008**, *130*, 5026–5027.
17. Mahler, B.; Spinicelli, P.; Buil, S.; Quelin, X.; Hermier, J.; Dubertret, B. Towards Non-blinking Colloidal Quantum Dots. *Nat. Mater.* **2008**, *7*, 659–664.
18. Malko, A. V.; Park, Y.-S.; Sampat, S.; Galland, C.; Vela, J.; Chen, Y.; Hollingsworth, J. A.; Klimov, V. I.; Htoon, H. Pump-Intensity- and Shell-Thickness-Dependent Evolution of Photoluminescence Blinking in Individual Core/Shell CdSe/CdS Nanocrystals. *Nano Lett.* **2011**, *11*, 5213–5218.
19. Park, Y.-S.; Malko, A. V.; Vela, J.; Chen, Y.; Ghosh, Y.; García-Santamaría, F.; Hollingsworth, J. A.; Klimov, V. I.; Htoon, H. Near-Unity Quantum Yields of Biexciton Emission from CdSe/CdS Nanocrystals Measured Using Single-Particle Spectroscopy. *Phys. Rev. Lett.* **2011**, *106*, 187401.
20. Donnert, G.; Eggeling, C.; Hell, S. Major Signal Increase in Fluorescence Microscopy through Dark-State Relaxation. *Nat. Methods* **2006**, *4*, 81–86.
21. Jacques, V.; Murray, J.; Marquier, F.; Chauvat, D.; Grosshans, F.; Treussart, F.; Roch, J. Enhancing Single-Molecule Photostability by Optical Feedback from Quantum Jump Detection. *Appl. Phys. Lett.* **2008**, *93*, 203307.
22. Nirmal, M.; Dabbousi, B.; Bawendi, M.; Macklin, J.; Trautman, J.; Harris, T.; Brus, L. Fluorescence Intermittency in Single Cadmium Selenide Nanocrystals. *Nature* **1996**, *383*, 802–804.
23. Zhao, J.; Nair, G.; Fisher, B. R.; Bawendi, M. G. Challenge to the Charging Model of Semiconductor-Nanocrystal Fluorescence Intermittency from Off-State Quantum Yields and Multiexciton Blinking. *Phys. Rev. Lett.* **2010**, *104*, 157403.
24. Rosen, S.; Schwartz, O.; Oron, D. Transient Fluorescence of the Off State in Blinking CdSe/CdS/ZnS Semiconductor Nanocrystals Is Not Governed by Auger Recombination. *Phys. Rev. Lett.* **2010**, *104*, 157404.
25. Galland, C.; Ghosh, Y.; Steinbrück, A.; Sykora, M.; Hollingsworth, J.; Klimov, V.; Htoon, H. Two Types of Luminescence Blinking Revealed by Spectroelectrochemistry of Single Quantum Dots. *Nature* **2011**, *479*, 203–207.
26. Stefani, F. D.; Knoll, W.; Kreiter, M.; Zhong, X.; Han, M. Y. Quantification of Photoinduced and Spontaneous Quantum-Dot Luminescence Blinking. *Phys. Rev. B* **2005**, *72*, 125304.
27. Peterson, J. J.; Nesbitt, D. J. Modified Power Law Behavior in Quantum Dot Blinking: A Novel Role for Biexcitons and Auger Ionization. *Nano Lett.* **2009**, *9*, 338–345.
28. Talapin, D.; Lee, J.; Kovalenko, M.; Shevchenko, E. Prospects of Colloidal Nanocrystals for Electronic and Optoelectronic Applications. *Chem. Rev.* **2010**, *110*, 389–458.
29. Carbone, L; Nobile, C.; De Giorgi, M.; Della Sala, F.; Morello, G.; Pompa, P.; Hytch, M.; Snoeck, E.; Fiore, A.; Franchini, I. R.; *et al.* Synthesis and Micrometer-Scale Assembly of Colloidal CdSe/CdS Nanorods Prepared by a Seeded Growth Approach. *Nano Lett.* **2007**, *7*, 2942–2950.